HARDI-Based Microstructural Complexity Mapping Reveals Distinct Subcortical and Cortical Grey Matter Changes in Mild Cognitive Impairment and Alzheimer's Disease

H. A. Haroon[1,2], H. Reynolds[1], S. F. Carter[2,3], K. V. Embleton[2,4], K. G. Herholz[2,3], and G. J. Parker[1,2]

[1]Imaging Science & Biomedical Engineering, School of Cancer & Enabling Sciences, The University of Manchester, Manchester, England, United Kingdom, [2]Biomedical Imaging Institute, The University of Manchester, Manchester, England, United Kingdom, [3]Wolfson Molecular Imaging Centre, School of Cancer & Enabling Sciences, The University of Manchester, Manchester, England, United Kingdom, [4]School of Psychological Sciences, The University of Manchester, Manchester, England, United Kingdom

Introduction There are many published studies of neurodegenerative conditions, such as Alzheimer's, involving diffusion MRI. However, these studies predominantly focus on properties of the white matter (e.g. fibre bundle trajectories, FA, MD, etc), e.g. [1]. It has previously been shown that it is possible to characterize grey matter diffusion complexity by obtaining probabilities of observing n distinct dominant diffusion orientations on a voxel-by-voxel basis[2,3] and that, for each n, the distribution of these probabilities within regions of cortical and subcortical grey matter reveals a signature of the underlying microstructure, influenced by the partial voluming of layering structure, and varying macroscopic contributions from white matter and CSF[4]. Here we apply this technique to groups of patients with mild cognitive impairment (MCI) and mild Alzheimer's disease (AD), and healthy controls (HC) of similar age. We find statistical differences in the regional median probabilities of observing n distinct dominant diffusion orientations between these subject groups providing evidence for the microstructural changes in grey matter associated with these pathologies.

Methods *Imaging:* High-resolution anatomical T_1-weighted data followed by HARDI were acquired in 7 HC (5F:2M, 70 years median age, range 60-73), 7 MCI (2F:5M, 70 years median age, range 65-83) and 7 AD (2F:5M, 77 years median age, range 71-86) on a 3 T Philips Achieva scanner (Philips Healthcare, Best, Netherlands) using an 8-element head coil. T_1: 3D Fast Field Echo Inversion Recovery with TE = 3.8 ms, TR = ~2000 ms, TI = 1150 ms, 256 × 205 matrix reconstructed to 256 × 256, reconstructed resolution 1 mm^3, 150 contiguous slices, SENSE factor = 2. HARDI: PGSE EPI with TE = 54 ms, cardiac gating, G_{max} = 62 mT/m, partial Fourier factor 0.679, 112 × 112 matrix reconstructed to 128 × 128, reconstructed resolution 1.875 × 1.875 mm^2, slice thickness 2.1 mm, 60 contiguous slices, 43 non-collinear diffusion sensitization directions at b = 1200 s/mm^2 (Δ = 29.8 ms, δ = 13.1 ms), 1 at b = 0, SENSE factor = 2.5, correction for susceptibility and eddy current-induced distortion[5]. *Cortical and Subcortical Parcellation:* We ran FreeSurfer's fully automated brain extraction, tissue segmentation[6] and parcellation[7] on the high-resolution T_1-weighted volume for each subject (surfer.nmr.mgh.harvard.edu). In each hemisphere we used 34 anatomically delineated cortical regions covering all of the cerebral cortex and 9 subcortical grey matter regions, defined using the aparc+aseg volume generated by FreeSurfer. The b = 0 volume for each subject was registered to the extracted T_1-weighted brain volume for that subject by implementing affine registration in FSL's (www.fmrib.ox.ac.uk/fsl) FLIRT[8]. The transformation matrix obtained was inverted and then applied to the parcellation volume from FreeSurfer, to register with each subject's HARDI data. *Constrained Spherical Deconvolution and MBR Bootstrapping:* As described in [3,4] with the exception that the dominant diffusion orientation distribution function was generated with 28 spherical harmonics (l_{max}=6)[9] here. *Probability of Number of Dominant Diffusion Populations:* The probability of observing n dominant diffusion orientations was determined over 100 MBR bootstrap iterations. *Probability Distribution in Parcellated Regions:* The median was calculated as the descriptor of the distribution of probabilities of n dominant diffusion orientations amongst all the voxels within each of the cortical and subcortical parcellated regions. *Statistical Testing:* We tested for any statistically significant difference in the median $P(n)$ for each n and for each of the cortical and subcortical regions between the groups of HC and MCI, and HC and AD, using the two-sided non-parametric Mann-Whitney U-test.

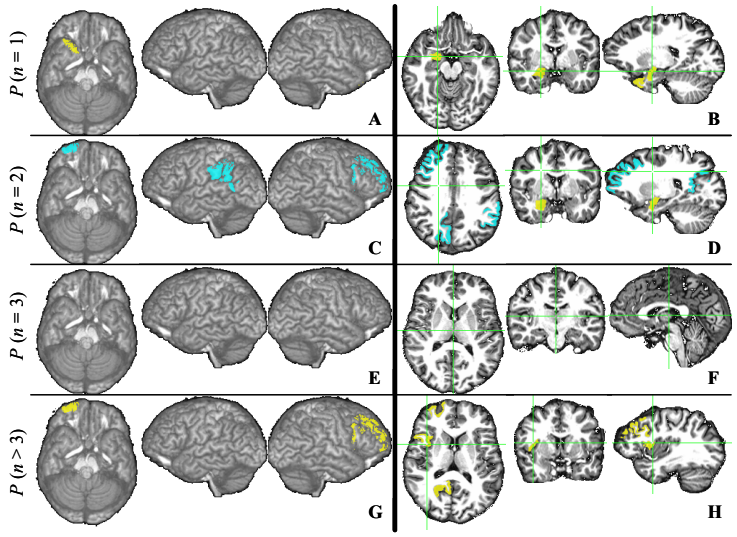

Fig 1: Significant group differences in regional median $P(n)$ between HC and MCI

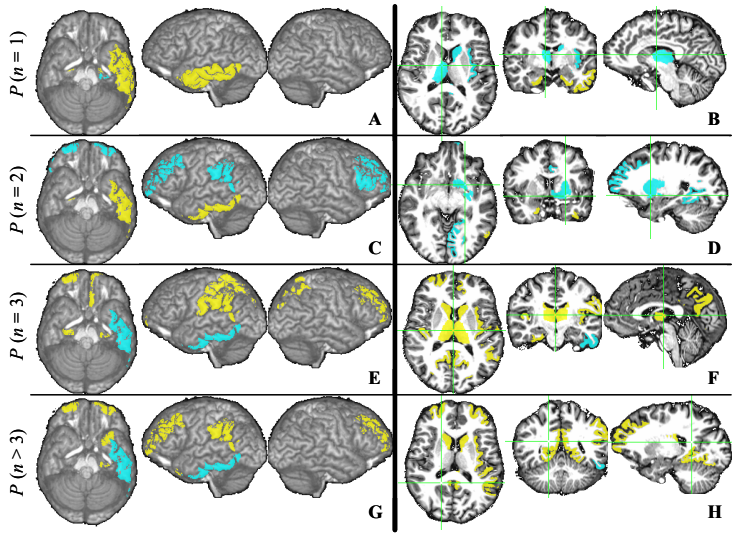

Fig 2: Significant group differences in regional median $P(n)$ between HC and AD

Results Renderings and orthogonal reconstructions (radiological convention) showing group differences are displayed in Figs 1 and 2. Subcortical and cortical grey matter regions showing statistically significant (p<0.05, not corrected for multiple comparisons) differences in $P(n)$, where $n \in [1, 2, 3, >3]$, between HC and MCI are shown in Fig 1, and between HC and AD are shown in Fig 2. Significant differences were also found between MCI and AD but the results are not shown here. Regions where the median $P(n)$ are significantly greater in HC than in MCI or AD are shown in yellow, and where the median $P(n)$ are significantly less in HC than in MCI or AD in blue. Significant differences in median $P(n=1)$ are displayed in Fig 1(A,B) and Fig 2(A,B); $P(n=2)$ in Fig 1(C,D) and Fig 2(C,D); $P(n=3)$ in Fig 1(E,F) and Fig 2(E,F); and $P(n>3)$ in Fig 1(G,H) and Fig 2(G,H). Median $P(n=3)$ showed no significant differences between HC and MCI (Fig 1(E,F)). There are more statistically significant differences between HC and AD than between HC and MCI, with the MCI differences generally appearing as a subset of the AD differences. **Conclusion** This work suggests that applying model-based residual bootstrapping to the CSD analysis of clinically-acquirable HARDI data can elucidate information about the underlying microstructural complexity of grey matter and that these methods are sensitive to degenerative disease of varying severity. We find that the degree of abnormality in grey matter complexity increases in AD relative to MCI, consistent with the concept of MCI being a prodromal state of AD. Although it is likely that macroscopic partial volume and atrophy will influence our results (via for example variations in CSF contamination), it is unlikely that our observations can be entirely explained by these effects as complexity changes are apparent in the subcortical grey matter where partial volume is negligible, suggesting that microstructural differences are also likely to be affecting our cortical findings.

References **1)** Bozzali M, *et al*, *NeuroImage*, in press, 2010. **2)** Haroon HA, *et al*, *IEEE Trans Med Imaging*, **28**:535, 2009. **3)** Haroon HA, *et al*, *ISMRM*, 363, 2009. **4)** Haroon HA, *et al*, *ISMRM*, 578, 2010. **5)** Embleton KV, *et al*, *Hum Brain Mapp*, **31**:1570, 2010. **6)** Han X, *et al*, *IEEE Trans Med Imaging*, **26**:479, 2007. **7)** Destrieux C, *et al*, *OHBM*, 541 SU-AM, 2009. **8)** Jenkinson M, *et al*, *NeuroImage*, **17**:825, 2002. **9)** Tournier J-D, *et al*, *NeuroImage*, **35**:1459, 2007.

Acknowledgements We would like to thank Shailendra Segobin for his help with data management. This work was supported by the UK's BBSRC (BB/E002226/1), MRC (G0501632), and a Summer 2010 Vacation Scholarship from The Wellcome Trust.